International Journal of Physical Sciences Vol. 7(46), pp. 6034-6043, 9 December, 2012
Available online at http://www.academicjournals.org/IJPS
DOI: 10.5897/IJPS12.285
ISSN 1992 - 1950 ©2012 Academic Journals

Full Length Research Paper

Compositional domain dynamics in two-coupled lipid monolayer: A mean field approximation approach

Kan Sornbundit[1], Waipot Ngamsaad[2], Charin Modchang[1,4], Narin Nuttavut[1,4], Darapond Triampo[3,4] and Wannapong Triampo[1,4,5]*

[1]R&D Group of Biological and Environmental Physics, Department of Physics, Faculty of Science, Mahidol University, Bangkok 10400, Thailand.
[2]School of Science, University of Phayao, Mueang Phayao, Phayao 56000, Thailand.
[3]Department of Chemistry, Center of Excellence for Innovation in Chemistry, Faculty of Science, Mahidol University, Bangkok 10400, Thailand.
[4]ThEP Center, CHE, 328 Si Ayutthaya Road, Bangkok 10400, Thailand.
[5]Institute for Innovative Learning, Mahidol University, 999, Phuttamonthon 4 Road, Salaya, Nakhon Pathom 73170, Thailand.

Accepted 12 November, 2012

A continuum model for artificial membrane was developed by treating the upper and lower layers of the membrane as a pair of coupled Ising monolayers. Linear coupling between the layers was included. Linear stability analysis was used to predict the phase diagram. The dependence of the phase-separated regions on inter-layer coupling is determined. We numerically solve the Cahn-Hilliard type equations to obtain domain evolutions for both layers. The estimations of the coupling strengths between the bilayers are determined from simulations. The dynamic scaling of the characteristic domain sizes for the symmetric and asymmetric cases are also evaluated from the simulations. Unique domain-growth scaling is reported in both cases.

Key words: Lipid bilayers, domain coarsening dynamics, mean-field approximation, inter-layer coupling estimation.

INTRODUCTION

Phase separation in model membranes, such as giant unilamellar vesicles (GUVs), is a challenging topic in biophysics (Veatch and Keller, 2002, 2003, 2005; Honerkamp-Smith et al., 2008, 2009). GUVs consist of two opposing lipid monolayer. Each monolayer generally contains three components: saturated lipids, unsaturated lipids, and cholesterol. At temperatures above the critical temperature (T_c), all of the lipid components in the vesicles are mixed, the vesicles appear to have a single phase. At temperatures below the critical temperature, the lipids on the membrane surface are laterally separated to small patches (or domains). These domains will gradually merge until reach the one-biggest domain so that the saturated lipids have preferential affinity to pack with cholesterol. The domains consisting of saturated lipids and cholesterol are usually called liquid-ordered (l_o) phase, while the region of unsaturated lipids are usually called liquid-disordered (l_d) phase.

Recent experiments (Collins and Keller, 2008; Kiessling et al., 2009; Wan et al., 2008) show the existence of coupling between the monolayers. The lipid domains in one layer can promote the formation of coherent domains in the opposing monolayer. If the lipid bilayers are prepared such that, both layers have the same lipid composition, then, complete domain registration would be observed. Three coupling mechanisms have been proposed (May, 2009). The first mechanism is based on electrostatic coupling due to the repelling force that occurs between the electrostatic charges in the

*Corresponding author. E-mail: wtriampo@gmail.com.

hydrophilic head of the phospholipids for each layer. This repelling force reduces the strength of the coupling, but it is generally negligible. The second mechanism involves cholesterol flip-flop (rapid movement of cholesterol between the monolayers). The third mechanism is dynamic chain interdigitation due to the overhanging of the lipid tails between the opposing layers. May (2009) show that coupling could be dominated by the third mechanism.

In the past decade, the interaction across the bilayer (or coupling) has received more attention. Estimating the coupling strength between monolayer is an active issue. According to May (2009), the coupling strength is defined by $\Lambda = \gamma a \Big/ \left(k_B T (\phi - \psi)^2\right)$ where $\phi, \psi, \gamma, a \approx 0.6\, nm^2$ are the order parameters of the upper layer, the order parameters of the lower layer, the mismatch energy and the average cross-sectional area per lipid. Hence, the mismatch energy can be used to calculate the strength of coupling. The coupling strengths between monolayers were first theoretically predicted by Collins (2008) to be 0.1 to 1, corresponding to $\gamma \approx 0.1 - 1\ k_B T / nm^2$. However, May (2009) argued that this range seems to be an overestimation. Related work by Risselada and Marrink (2008) used molecular dynamics simulations to determine the coupling strength. Their estimate for coupling was $\Lambda = 0.1 - 0.2$, which correspond to $\gamma = 0.15 k_B T / nm^2$. Wagner et al. (2007) determined a formula for calculating the critical coupling strength, Λ^*, separating two and three phase regions. The two- and three-phase regions correspond to the matched and mismatch regions when the bilayer is observed from the top view. Wagner et al. (2007) showed that the value of Λ^* can be in the order of 0.47, a bit larger than the estimation of Risselada and Marrink (2008). Recent work by Putzel et al. (2011) calculated the mismatch energy by using the molecular mean field approach. The mismatch energies calculated by this method are approximately $\gamma \approx 0.01 - 0.03 k_B T / nm^2$. They did not converse the mismatch energies to the coupling strengths, but it must be lower than that obtained by Risselada and Marrink (2008). A comprehensive review by Almeida (2009) stated that coupling across the bilayer is approximately -100 cal/mol or around 0.169 $k_B T$ at room temperature. This value lies within the range of Risselada and Marrink (2008). Therefore, the strengths of coupling are still controversial.

To the best of our knowledge, only the work of Wagner et al. (2007) can be applied to the systems that have different lipid composition on bilayer. Otherwise, the calculations are based on the situation that lipid bilayers have the same lipid compositions. From the literature, you may see that the certain value (or even range) of the coupling strength is rather confusing. In this work, we use simulations, which are based on our model, to estimate the coupling strength for either the same and different lipid composition.

An interesting question about model membrane systems is whether there are scaling laws for domain coarsening. Scaling laws have been investigated experimentally and computationally, but the reported results are conflicting. Saeki et al. (2006) measured the domain dynamics in cell-sized liposomes and found the relationship $R(t) \sim t^{0.15}$ for off-critical mixtures. Yanagisawa et al. (2007) performed experiments on ternary model membranes and found two coarsening regimes. The first regime is the normal coarsening, which is governed by $R(t) \sim t^{2/3}$. The second regime is called trapped coarsening, which means that domain coarsening is suppressed beyond a critical domain size. Liang et al. (2010) also performed experiments on ternary model membranes and reported that domains initially coarsen as $R(t) \sim t^{1/3}$. After 10 to 100 s, the rate of coarsening increases to be $R(t) \sim t$. Laradji and Kumar (2004, 2006) used dissipative particle dynamics (DPD) method to investigate the growth dynamics of lipid bilayers. They found that the domains, for both symmetric and asymmetric cases, first evolve with rate $R(t) \sim t^{0.3}$. After a turning point, the growth rates depend strongly on area-to-volume ratios of vesicles. Ramachandran et al. (2010) simulated a sheet of membrane embedded in a bulk fluid by using the DPD method. They found the growth rate $R(t) \sim t^{1/3}$ for either critical or off-critical compositions. Camley and Brown (2011) also simulated membranes in a bulk fluid using Cahn-Hillird (CH) typed equation. They observed the rate $R(t) \sim t^{1/2}$ for critical composition and the rate $R(t) \sim t^{1/3}$ for off-critical composition. The lattice-based model has also been used to study the domain growth dynamics. Gómez et al. (2008) proposed two interconnected lattices for modeling a lipid membrane. They obtained the dynamic scaling law in the form $R(t) \sim t^{1/3}$ for the late stage. Recently, Ehrig et al. (2011) found that the growth dynamics depend on the lipid composition and temperature. They reported that the growth dynamics are $R(t) \sim t^n$ where $n \approx 1/4 - 1/3$. Therefore, the domain coarsening law remains unresolved.

The main goals of this research are to estimate the interlayer coupling strength and investigate the dynamic scaling law of the domains. Linear stability analysis is used to investigate the phase diagrams. The coupling strengths are evaluated by comparing simulations with experiments. We have found that our possible coupling strength ranges differ from previous estimations. A pair of Cahn–Hilliard-type equations for each monolayer are developed and used to simulate the systems. The dynamic scaling laws of the domains are determined from the simulations.

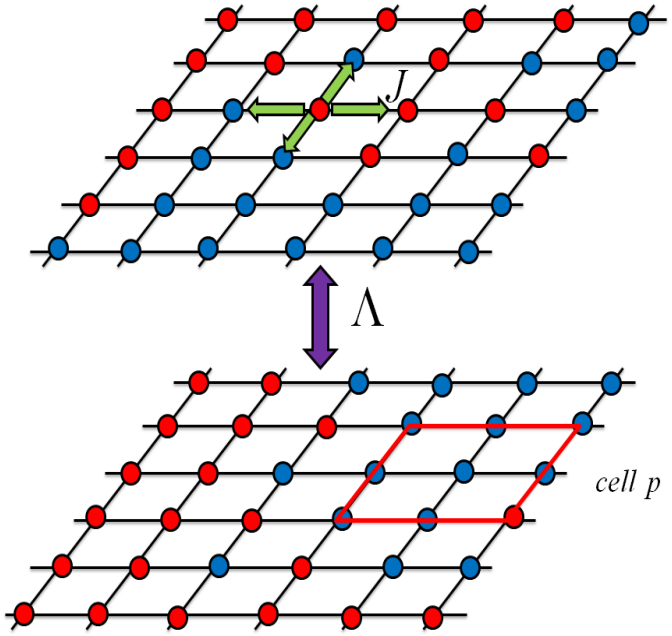

Figure 1. Schematic of a lipid bilayer used in this work. Red and blue circles represent particle A and B, respectively. The upper and lower lattices represent upper and lower lipid monolayers. The intra-layer interactions of a particular particle are denoted by J, and the inter-layer interaction (or coupling) of a pair of particles that localizes to the same position on opposing monolayers is denoted by Λ.

METHODOLOGY

Model and kinetics equations

We develop a model to include the effect of inter-layer interaction (or coupling) between two layers which have received less attention in the past. The structural basis of model membranes is two lipid monolayers that are coupled in some way. Therefore, the systems are modeled as two opposed, fully filled planar square lattices that are Ising monolayers, as shown in Figure 1. One monolayer is the upper layer, and the other is the lower layer. Each layer consists of a binary mixtures species *A* and *B* representing the two liquid phases l_o and l_d, respectively. Particle *A* is a tight binding state (or complex) of the saturated lipid and cholesterol, and the unsaturated lipid is particle *B*. The coupling between the layers is represented by the interaction of a pair of particles located opposite each other in the layers. Since we assume that lipid or cholesterol molecules exchange between the bilayer and environment are not allowed, then the amount of lipids and cholesterol are conserved.

According to Hohenberg and Halperin (1977), the model can be classified to the class of model B.

The Hamiltonian of the system is a combination of the Hamiltonians corresponding to the upper layer (H^t), the lower layer (H^b) and interlayer interactions (H^Λ). It is given by:

$$H^{tot} = H^t + H^b + H^\Lambda = -J\sum_{\langle ij\rangle} U_i U_j - J\sum_{\langle ij\rangle} L_i L_j - \Lambda\sum_i U_i L_i, \quad (1)$$

Where the total Hamiltonian of the system is H^{tot}. U_i and L_i are the particles that reside on the upper and lower layers, respectively, at site i. Particle values of +1 or -1 denote the occupation at site *i* by *A* or *B*, respectively. The neighboring particle-particle interaction strength is represented by $J>0$, and it corresponds to the preferential affinity for a like component. The summations in the first two terms denote the sum of the nearest-neighbor particles. The strength of the interlayer coupling is represented by the parameter $\Lambda>0$. The summation in the last term denotes the sum of all interactions between two opposed particles, one on the top layer and another one on the bottom layer.

Extracting information analytically from a model in the Ising-like form is difficult. However, the Ginzberg-Landau free energy can be used to explain most phase-separating systems, and a large amount of information can be derived from it. The Ginzberg-Landau free energy is written as powers of the order parameters. Such free energy can be deduced from our Ising-like model by using the mean field approximation. To do so, each lattice is partitioned into smaller sub-partitions (called cells), labeled by index p, (Figure 1). Note that, cell p in Figure 1 is drawn for a guide line. It does not contain only 9 particles. We assume that the cells are large enough to contain many particles and are very small when compared with the size of the systems. The energy of a particular subsystem, E_p, is defined as a combination of energies of one cell on the top layer, a coherent cell on the other layer and a transbilayer interaction term. It is defined in terms of the unit k_BT (where k_B is Boltzmann's constant and T is absolute temperature) as:

$$E_p = -J\sum_{\langle ij\rangle\in p} U_i U_J - J\sum_{\langle ij\rangle\in p} L_i L_J - \Lambda\sum_{i\in p} U_i L_i, \quad (2)$$

Where the summations denote the sum within cell p. The order parameters in the subsystems are called the average field variables. They are given as follows:

$$\phi(\vec{r}_p) = \sum_{i\in p} U_i = \frac{N_A^U - N_B^U}{N_{AB}^U}, \psi(\vec{r}_p) = \sum_{i\in p} L_i = \frac{N_A^L - N_B^L}{N_{AB}^L} \quad (3)$$

Where N_j^X is the number of species j in cell p of the upper layer (the superscript $X=U$) or the lower layer (the superscript $X=L$). The parameters $\phi(\vec{r}_p)$ and $\psi(\vec{r}_p)$ represent the order parameter for a particular cell (called cell p) on the top and an opposed cell on the bottom layer, respectively. N_{AB}^X is the total number of particles in cell p, $N_{AB}^X = N_A^X + N_B^X$. The effect of the neighboring particles is approximated as the product of the number of neighboring particles, z (for this work, $z=4$ corresponds to a square lattice), and the averaged field variable, that is, the neighboring particles are replaced by the averaged value of the particles. The energy of the cell p on the upper layer is:

$$\begin{aligned} E_p^t &= -J\sum_{\langle ij\rangle\in p} U_i U_j = -J\sum_{i\in p} U_i \left(\text{summation of neighboring spins}\right) \\ &\approx -\frac{1}{2}J\sum_{i\in p} U_i z\phi(\vec{r}_p) = -\frac{1}{2}Jz\phi(\vec{r}_p)\sum_{i\in p} U_i = -\frac{1}{2}zJ\phi(\vec{r}_p)\times\phi(\vec{r}_p) \\ &= -\frac{1}{2}zJ\phi(\vec{r}_p)^2. \end{aligned} \quad (4)$$

The factor $1/2$ is added to avoid the double counting. The same approximation is applied to the lower layer. The energy due to the coupling between both layers at cell p is:

$$E_p^{\Lambda} = -\Lambda \sum_{i \in p} U_i L_i. \quad (5)$$

With the Bragg-Williams approximation, spin configurations in cell p are represented by one parameter which is called order parameter. Therefore, we assume that the product of individual spin in cell p are represented by the product of the order parameter of cell p as follows:

$$E_p^{\Lambda} = -\Lambda \sum_{i \in p} U_i L_i \approx -\Lambda \phi(\vec{r}_p)\psi(\vec{r}_p) \quad (6)$$

The bulk free energy per cell is expressed by:

$$f_p\left[\phi(\vec{r}_p),\varphi(\vec{r}_p)\right]/k_B T = -\frac{1}{2}J'\phi^2 + \frac{1}{2}\left[(1-\phi)\ln(1-\phi)+(1+\phi)\ln(1+\phi)\right] - \frac{1}{2}J'\psi^2 + \frac{1}{2}\left[(1-\psi)\ln(1-\psi)+(1+\psi)\ln(1+\psi)\right] - \Lambda'\phi\psi - 2\ln 2. \quad (7)$$

Where $J' = zJ$ and $\Lambda' = \Lambda/k_B T$. In the vicinity of the critical temperature (where ϕ and ψ are very small), this free energy can be rewritten as:

$$f_p\left[\phi(\vec{r}_p),\psi(\vec{r}_p)\right]/k_B T \approx -\frac{(J'-1)}{2}\left(\phi^2+\psi^2\right) + \frac{1}{12}\left(\phi^4+\psi^4\right) - \Lambda'\phi\psi. \quad (8)$$

Note that, in the absence of coupling, the free energy splits into two free energies according to each monolayer. The total free energy functional is integral to the overall cells and is defined by:

$$F[\phi,\psi] = \int ds \left\{ f_p + \frac{\kappa}{2}\left[(\nabla\phi(\vec{r}_p))^2 + (\nabla\psi(\vec{r}_p))^2\right]\right\}, \quad (9)$$

Where $\kappa > 0$ is an interfacial parameter. The first term in the integral is the bulk free energy, and the square-gradient terms are the energies associated with non-uniform domain distributions. The line tension between the phases is related to the parameter κ by $\sigma = (2\sqrt{2})/9\kappa^{1/2}(J'-1)^{3/2}$. The pair of coupled Cahn-Hilliard equations that describe the temporal patterns for each layer are expressed as follows:

$$\frac{\partial\phi}{\partial t} = M\nabla^2 \frac{\partial F(T,\phi,\psi)}{\partial\phi} = M\nabla^2\left[(1-J')\phi + \phi^3/3 - \kappa\nabla^2\phi - \Lambda'\psi\right] \quad (10)$$

$$\frac{\partial\psi}{\partial t} = M\nabla^2 \frac{\partial F(T,\phi,\psi)}{\partial\psi} = M\nabla^2[(1-J')\psi + \psi^3/3 - \kappa\nabla^2\psi - \Lambda'\phi], \quad (11)$$

Where M is the diffusivity of lipid.

Linear stability analysis

We can extract a useful relationship from a linear stability analysis of the kinetic Equations 10 to 11. We tested the stability of the homogeneous solution (ψ_0, φ_0) by adding small perturbations $\delta\phi = \exp[\lambda(q)t + iqx]$ and $\delta\psi = \exp[\lambda(q)t + iqx]$. We first define

$$\phi = \phi_0 + \delta\phi \quad (12)$$

$$\psi = \psi_0 + \delta\psi \quad (13)$$

Next, we substituted Equations 12 to 13 into Equations 10 to 11, and then, Taylor expanded up to the first order. Finally, we obtain the linearized equations, as follows:

$$\frac{\partial\delta\phi}{\partial t} = M\nabla^2\left[\left(1-J'+\phi_0^2\right)\delta\phi - \Lambda'\delta\psi - \kappa\nabla^2\delta\phi\right] \quad (14)$$

$$\frac{\partial\delta\psi}{\partial t} = M\nabla^2\left[\left(1-J'+\psi_0^2\right)\delta\psi - \Lambda'\delta\phi - \kappa\nabla^2\delta\psi\right] \quad (15)$$

with the constraints

$$(1-J')\phi + \frac{1}{3}\phi^3 - \Lambda'\psi = 0 \quad (16)$$

$$(1-J')\psi + \frac{1}{3}\psi^3 - \Lambda'\phi = 0 \quad (17)$$

Substituting the small perturbations into Equations 14 to 15, we obtain the following matrix equation:

$$\begin{pmatrix} -Mq^2[1-J'+\phi_0^2+\kappa q^2] & \Lambda' Mq^2 \\ \Lambda' Mq^2 & -Mq^2[1-J'+\psi_0^2+\kappa q^2] \end{pmatrix}\begin{pmatrix}\delta\phi \\ \delta\psi\end{pmatrix} = 0 \quad (18)$$

The growth rate function, $\lambda(q)$, is the largest eigenvalue obtained from Equation 18. The growth rate is:

$$\lambda(q) = -\frac{1}{2}Mq^2\left(2(1-J'+\kappa q^2)+\phi_0^2+\psi_0^2 - \sqrt{4\Lambda'^2+\left(\phi_0^2-\psi_0^2\right)^2}\right) \quad (19)$$

The plots of $\lambda(q)$ versus Λ' for condition $\phi_0 = \psi_0 = 0$ and $J' = 3.2$ are shown in Figure 2.

The wave numbers q that make positive growth rate function are the unstable modes. The wave numbers q that make negative growth rate function are the stable modes. The unstable mode means that phase separation occurs. A useful relation can be determined by considering the wave numbers at which the growth rate function becomes negative. The growth rate function vanishes at $q = 0$ and $q = q_0$,

Where

$$q_0^2 = \frac{-2+2J'-\phi_0^2-\psi_0^2+\sqrt{4\Lambda'^2+\left(\phi_0^2-\psi_0^2\right)^2}}{2\kappa}. \quad (20)$$

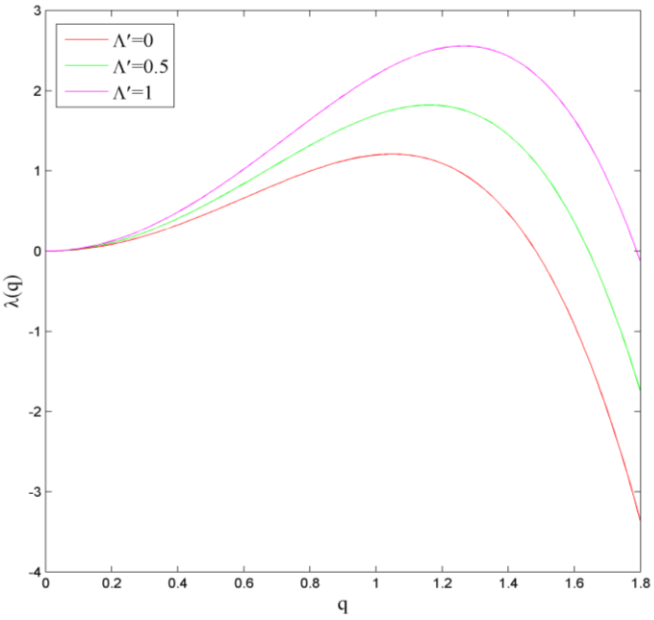

Figure 2. A plot of the growth rate function for the critical symmetric condition, $(\phi_0,\psi_0)=(0,0)$, with different couplings.

The right-hand side of Equation 20 must be positive, so the right-hand side can be written as:

$$\frac{-2+2J'-\phi_0^2-\psi_0^2+\sqrt{4\Lambda'^2+\left(\phi_0^2-\psi_0^2\right)^2}}{2\kappa}>0. \quad (21)$$

We can use Equation 21 to derive the critical value of $J'(J'_C)$ as a function of lipid compositions and the interlayer coupling. This relationship can be expressed as:

$$J'_C=\frac{1}{2}\left(2+\phi_0^2+\psi_0^2-\sqrt{4\Lambda'^2+\left(\phi_0^2-\psi_0^2\right)^2}\right). \quad (22)$$

In the single-layer case $\Lambda'=0$, the famous relationships $J_c=\left(1+\phi_0^2\right)/z$ and $J_c=\left(1+\psi_0^2\right)/z$ are archived. These are the critical values for J in a binary mixture system. The plots of J'_C versus Λ' for the critical composition $\phi_0=\psi_0=0$ are shown in Figure 3.

Figure 3 shows how the critical value of J'_C depends on the strength of interlayer coupling Λ'. The areas above the lines are the phase-separated regions, while the areas below the lines are the homogeneous regions. Figure 3 shows that at a particular coupling strength the minimum strength of J' required for phase separation in critical symmetric case is lower than that in asymmetric case.

Another point is that when coupling is larger, the critical strength of J' for phase separation is lower. Moreover, the relationship is linear when the lipid compositions on both layers are the same.

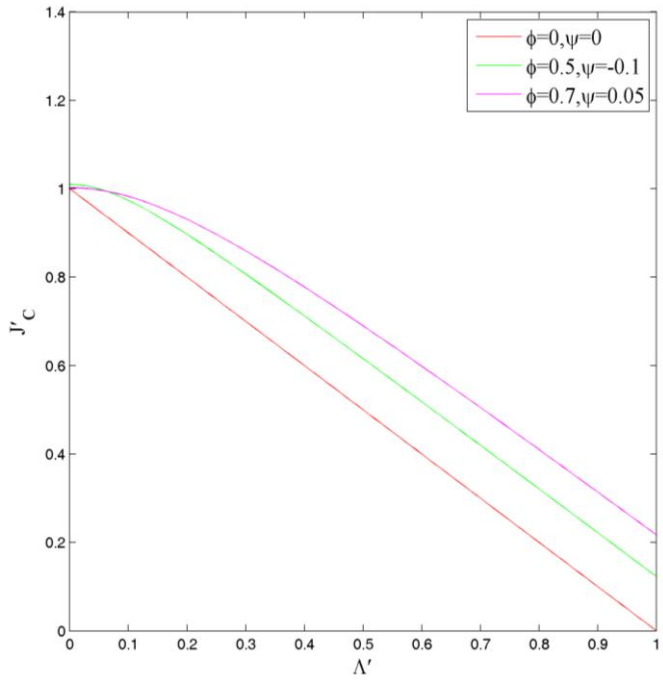

Figure 3. A plot of the critical values of J'_C as a function of Λ' for different initial conditions

Simulation details

To obtain morphological patterns, we have solved Equations 10 to 11 numerically by using the finite-difference method. The discretized version of those equations are expressed by:

$$\phi_{i,j}^{k+1}=\phi_{i,j}^{k}+\frac{M\Delta t}{(\Delta x)^2}\nabla_{i,j}^2[-r\phi_{i,j}^{k}+u\left(\phi_{i,j}^{k}\right)^3-\kappa\nabla_{i,j}^2\phi_{i,j}^{k}-\Lambda'\psi_{i,j}^{k}], \quad (23)$$

$$\psi_{i,j}^{k+1}=\psi_{i,j}^{k}+\frac{M\Delta t}{(\Delta x)^2}\nabla_{i,j}^2[-r\psi_{i,j}^{k}+u\left(\psi_{i,j}^{k}\right)^3-\kappa\nabla_{i,j}^2\psi_{i,j}^{k}-\Lambda\phi_{i,j}^{k}], \quad (24)$$

Where the discretized Laplacian operator is defined for a generic function as:

$$\nabla_{i,j}^2 y_{i,j}=y_{i+1,j}+y_{i-1,j}+y_{i,j+1}+y_{i,j-1}-4y_{i,j}.$$

All of the simulations have been performed on lattices of size $N\times N=512\times512$, with a periodic boundary condition. The compositional fields are defined in the site $i,j\in[1,N]$, and the iteration index is defined by k. The total time lapse up to iteration k then becomes $t=k\Delta t$. To ensure the Von Neumann stability criteria, the simulation parameters are chosen to be $\Delta t=10^{-3}$ and $\kappa=1$. We choose the simulation length unit $(s.l.u.)$ to be $\Delta x=1$ as a unit of the interfacial width, representing a physical size of approximately $5\,nm$. The diffusivity M is chosen to be 1 in

a unit of $(simulation\ length\ unit)^2/(simulation\ time\ unit)$ or $(s.l.u.)^2/(s.t.u.)$. All of the systems have been initially prepared in a homogeneous state. The simulations are started by adding a small perturbed distribution to each site. The intra-layer interaction in the simulations is $J' = 3.2$ and corresponds to the temperature below the critical temperature of the classical Ising model (Onsager, 1944). The strengths of the interlayer coupling are varied as $\Lambda \in (0,1)$. These probable values of the coupling are compiled from earlier estimations.

RESULTS AND DISCUSSION

Here, we show snapshots of characteristic domain evolutions for different membrane compositions. The rough estimation of the coupling strength for the symmetric and asymmetric cases can be obtained by comparing these snapshots with the experimental results. Then, the compositional domain scaling dynamics were investigated.

Coupling strength estimation

Here, we propose another way for estimating the coupling strength. We use simulation method based on our Cahn-Hilliard-typed equations and compare the simulations with experimental results. Two experimental scenarios must be reproduced from the simulations. First, the domain strips on both layers would be completely registered if the compositions of both layers are the same. The second scenario is the three-phase region that would be obtained if the lipid compositions of both layers are different. The three-phase region consists of registered regions of each phase and the unregistered region. These mimic the l_o/l_o, l_d/l_d and l_o/l_d interfaces between two layers in model membranes. We have performed the simulations for the critical symmetric and asymmetric cases with the coupling strength ranging from $\Lambda' = 0.02 - 0.5$. This choice is based on previous estimations. The results are shown and are discussed

Symmetric bilayer

In the experiments, the lipid domains on both monolayers register completely - either critical or off-critical compositions. This situation must be reproduced by the simulations. For this case, we have performed simulations in the bilayers which have critical composition on both layers. It means that both layers are initially prepared in the composition $\phi_0 = \psi_0 = 0$. The simulation results for this case are shown in Figure 4. Here, we should clarify the meaning of the colours in the figures.

All of the figures in this section show the top view of the bilayers. The red and blue regions represent matched (or registered) regions, and the green regions represent mismatch (or unregistered) regions.

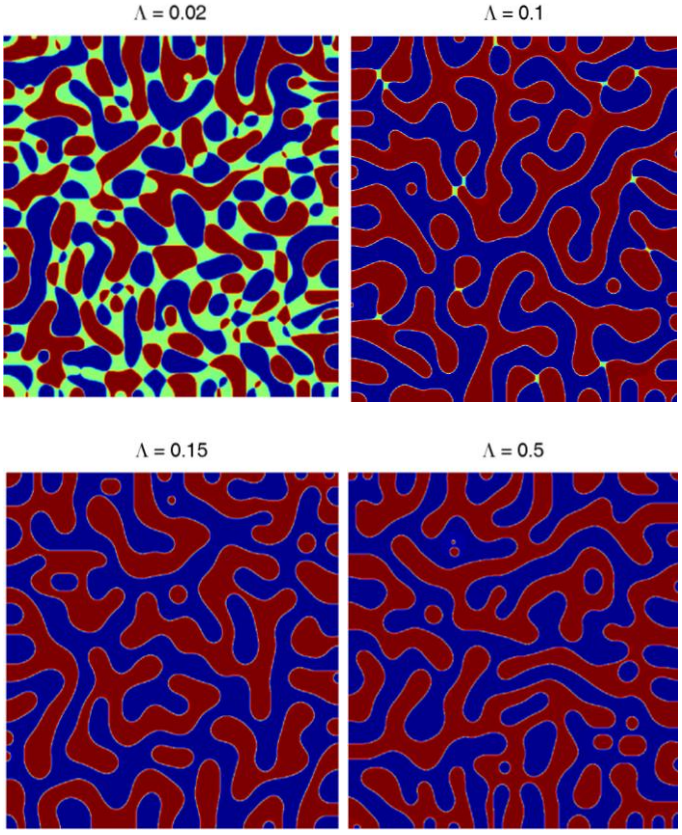

Figure 4. Snapshots of the phase morphologies in critical symmetric bilayers at the time unit 6 × 10^6 for different interlayer couplings.

From Figure 4, the complete domain registration, which reflects real situations, is found since the coupling strength is 0.15. On the other hand, the three-phase regions (red, blue and green) are produced at the coupling strength 0.02. This indicates that the strength 0.02 is not sufficiently large to induce the proper patterns. Therefore, the minimum coupling for this case should be approximately 0.15. This value has the same order as the previous predictions by Collins (2008) and Risselada and Marrink (2008). It should be noted that our method does not provide an estimated maximum coupling strength for this case.

Asymmetric bilayer

The asymmetric bilayer means that each monolayer has a different lipid composition. It is straightforward to expect that the three-phase regions must be observed. Interestingly, three-phase regions can be observed for some of the coupling strengths. We have performed simulations for the bilayer with $\phi_0 = 0.7, \psi_0 = 0.05$ (system I),

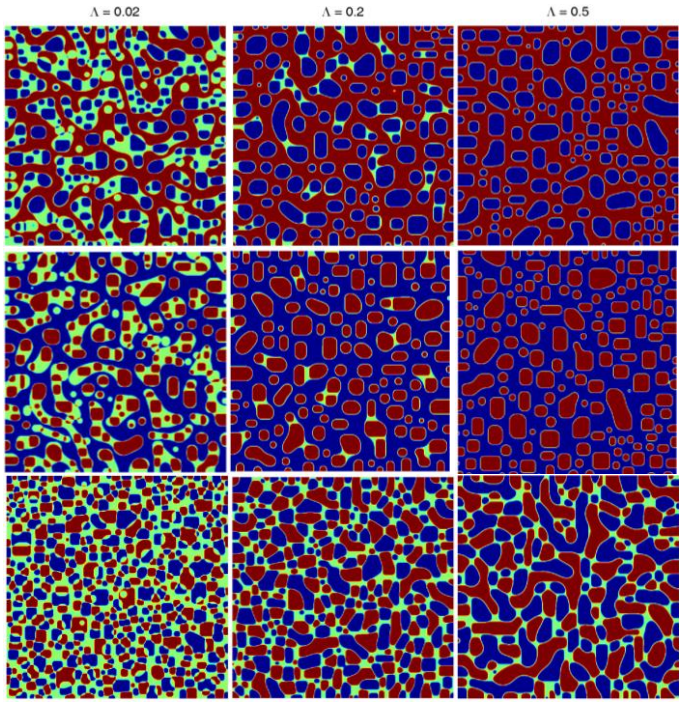

Figure 5. Snapshot of the phase morphologies in asymmetric bilayers at time unit 6 × 10^6 for different interlayer couplings. The lipid compositions for the first, second and third panels are $(\phi_0, \psi_0) = (0.7, 0.05), (-0.1, -0.7)$ and $(0.6, -0.6)$, respectively.

$\phi_0 = -0.1, \psi_0 = -0.7$ (system II) and $\phi_0 = 0.6, \psi_0 = -0.6$ (System III). The simulation results are shown in Figure 5.

For Systems I to III, the coupling strengths 0.02 to 0.2 induce the simulation patterns that are similar to experimental results, and exhibit three-phase regions. This reflects experimental situations. At the coupling strength 0.5, the System I to II exhibit only two-phase regions, even if they are initially prepared in different compositions. It does not capture the real situations. However, these abnormal situations are previously predicted by Wagner et al. (2007). Some results of Wagner et al. (2007) are discussed here. In their phase diagrams (Figure 3 in their paper), the coupling strength is 0.02 reflecting real situations more than the other values. In Wagner et al. (2007) diagram, the symmetric bilayers show two-phase regions, while the asymmetric bilayers show three-phase regions (the areas within the triangles). At larger coupling strengths (larger than 0.02), the three-phase regions are reduced. This allows the present of two-phase regions; even both layers have different lipid compositions. At the coupling strengths larger than 0.47, all preparation provide only two-phase regions, for the value of non-ideality of the binary mixture is 2.2. Therefore, in order to produce a reasonable phase separation, the coupling strengths should be on the order of 0.02. For our result in System III, the three-phase regions are observed at the coupling 0.02, 0.2, and 0.5. This means that the probable coupling strength for the asymmetric case depend strongly on the lipid distributions on each layer. Moreover, the strengths of coupling can be in the order of 0.5. It is larger than the maximal coupling strength from the results of Wagner et al. (2007) for the non-ideality of the binary mixture is 2.2. The results about the coupling strength estimations are summarized in Table 1.

Compositional domain dynamics

We investigate domain coarsening dynamics on both layers. The averaged domain size at a given time $R(t)$ is calculated by using the correlation function at different times for ϕ and ψ fields. The correlation function for the ϕ field at a time t and a distance $\vec{r}$ from the reference site $\vec{r}'$ is defined by:

$$C(\vec{r},t) = \frac{\langle \phi(\vec{r}',t)\phi(\vec{r}'+\vec{r},t)\rangle - \langle \phi(\vec{r}',t)\rangle^2}{\langle \phi(\vec{r}',t)^2\rangle - \langle \phi(\vec{r}',t)\rangle^2}, \quad (25)$$

Where the brackets are the average over all positions $\vec{r}'$. The distance $|\vec{r}| = R$ satisfying the condition $C(R,t) = 0$ is the average radius of domains. This method is also applied for the φ field. The results are shown and are discussed below.

Symmetric bilayer

We have performed simulations with initial composition $\phi_0 = 0, \psi_0 = 0$ with $\Lambda = 0.2$ and 0.5 as shown in Figure 6a and b. In this figure, the averaged domains sizes on both layers are evolved by the law $R(t) \sim t^n$, where $n \approx 1/3$. Note that, all data points of both layers are completely overlapped because domains on both layers are developed in the same patterns, (Figure 6a and b). The complete overlap of domains can be observed in previous experiments on symmetric bilayers. Moreover, the coupling strengths do not affect the coarsening rate. With the coupling strengths $\Lambda = 0.2$ and 0.5, the dynamics length scales are the same. Domains evolving with the law $R(t) \sim t^{1/3}$ suggest that domains grow by collision and coalescence mechanism.

Our results can be compared with those experiments of Liang et al. (2010) in the early stage. They reported that domain grow with the rate $R(t) \sim t^{1/3}$ for 10 to 100 s. For the late stage, domains grow faster than the early stage

Table 1. Summary of the previous coupling strength Λ estimations according to the definition of May (2009), except for Putzel et al. (2011).

Author	The mismatch energy γ	The estimated coupling strength Λ	Remark
Collins (2008)	$\gamma \approx 0.1-1\, k_B T/nm^2$	$\Lambda \approx 0.1-1$	Neglects the electrostatic effect between head group of lipids
Risselada and Marrink (2008)	$\gamma \approx 0.15\, k_B T/nm^2$	$\Lambda \approx 0.1-0.2$	The coupling are calculated by fitting with the probability distribution of the mismatch areas
Putzel et al. (2011)	$\gamma \approx 0.01-0.03\, k_B T/nm^2$	They do not calculate the coupling strengths.	Calculate analytically by using molecular theory
Our results	We do not calculate the mismatch energies.	1) symmetric case: the minimum strength is $\Lambda_{\min} \approx 0.15$ 2) asymmetric case: the coupling strength vary with lipid compositions	Compare the simulation results with the experimental results

Our results are also compared with the earlier results.

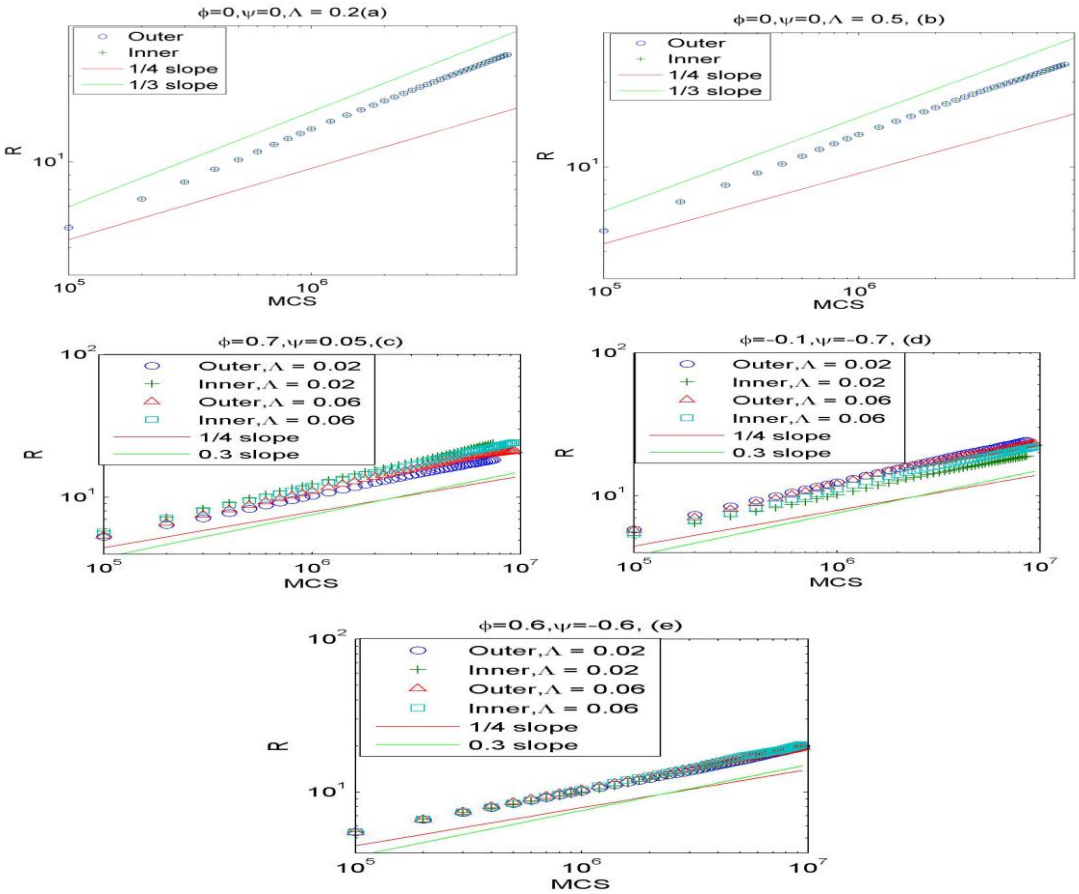

Figure 6. Log-Log plots of the time evolution of the characteristic domain sizes for symmetric (a-b) and asymmetric cases (c-e). Circles and triangles are the data for the upper (outer) layer with $\Lambda = 0.02$ and 0.06, respectively. Crosses and squares are the data for the lower (inner) layer with $\Lambda = 0.02$ and 0.06, respectively. The lines with slope 1/4, 0.3 and 1/3 are drawn for visual comparisons.

Table 2. Summary of the previous domain growth dynamics estimations.

Author	Domain growth dynamics
Saeki et al. (2006)	Experiment: $R(t) \sim t^{0.15}$ for off-critical mixtures
Yanagisawa et al. (2007)	Experiment: $R(t) \sim t^{2/3}$ (normal coarsening) and trapped regime.
Liang et al. (2010)	Experiment: $R(t) \sim t^{1/3}$ (early stage), $R(t) \sim t$ (late stage)
Laradji and Kumar (2004, 2006)	Simulation: The dynamics depend on area-to-volume ratios
Ramachandran et al. (2010)	Simulation: $R(t) \sim t^{1/3}$ for both critical and off-critical compositions with Solvent
Gomez et al. (2008)	Simulation: $R(t) \sim t^{1/3}$ for the late stage
Ehrig et al. (2011)	Simulation: $R(t) \sim t^{n}$ where $n \approx 1/4 - 1/3$
Our results	Simulation: $R(t) \sim t^{n}$ where $n \approx 1/3$ for symmetric case and $n \approx 0.3$ for asymmetric case.

Our results are also compared with the earlier results.

with the rate $R(t) \sim t$ by collision-induced collision mechanism (CIC). This mechanism can be explained as follows:

When two domains collide and merge into one bigger domain, they generate hydrodynamics flow. The hydrodynamics flow will induce subsequent collisions of neighboring domains which make domains grow faster. However, these results differ from the experimental works of Yanagisawa et al. (2007). They concluded that some domains grow with the law $R(t) \sim t^{2/3}$ while some domains are trapped. Their explanation is that the law $R(t) \sim t^{2/3}$ occurs because domains grow in the presence of hydrodynamics. Furthermore, the repulsive forces between capped domains are the key to inhibit the coalescence of other domains. Liang et al. (2010) suggested that the different topology of domains yield the different growth dynamics. In our work, we do not include the effect of hydrodynamic flow and the topology of membrane surface, such as domain budding, in the model so we cannot observe the rate $R(t) \sim t$, $R(t) \sim t^{2/3}$ or domain stabilization. However, the computational works of Laradji and Kumar (2004, 2006) used the model that is able to include the effect of membrane topology but they did not observe the rate $R(t) \sim t$, $R(t) \sim t^{2/3}$ or domain stabilization. Moreover, the recent computational work of Ramachandran et al. (2010) and Camley and Brown (2011) that explicitly include the hydrodynamics flow in the model do not report the rate $R(t) \sim t$. Therefore, the domain coarsening dynamics are still debatable.

Note that although our model does not include the effect of hydrodynamics and the effect of membrane topology, it includes the effect of the coupling field between layers. For the symmetric case, the effect of the coupling field does not provide a significant difference from single layer but it will show clearly in the asymmetric case.

Asymmetric Bilayer

In the present, the vesicles with different lipid ratios on both layers can be made in a laboratory (Collins and Keller, 2008). Interestingly, to the best of our knowledge, there is no report about the dynamics length scale measurements in either experimental or computational works. Therefore, our work seems to be the first work to report about the domains coarsening dynamics on both layers. Figures 6c to e show that the averaged domain sizes on both layers develop with nearly the same rate. The coarsening rate at the late stage is $R(t) \sim t^{\alpha}$, where $\alpha \approx 0.3$. This rate is slightly lower than the rate in the symmetric case. Moreover, it agrees with the growth rate of the early stage obtained by Laradji and Kumar (2006). However, we do not consider the effect of the area-to-volume ratio so our results do not agree with their results in the late stages.

Unlike the symmetric case, the presence of coupling between layers induces domains in the same kind on each layer to transversely register. It yields the matched domains move within the mismatch domains (red or blue domains move within green domains). This event can be observed in experiments of asymmetric bilayers (Collins and Keller, 2008). Indeed, computational models that consider a membrane as a single-layered object cannot reproduce this phenomenon. The results about the domain growth dynamics measurements are summarized in Table 2.

Conclusion

This work investigates the phase diagrams and the compositional domain dynamics in lipid bilayers. The model is based on two coupled Ising monolayers. The free energy governing the system is derived by applying the mean-field approximation to the Ising bilayer.

The strength of the coupling can be roughly extracted by comparing the compositional domain morphologies from the simulations with the experimental results. We propose that the minimum coupling strength of the symmetric bilayer which has critical composition on each layer is approximately 0.15. For the asymmetric case, with the compositions used in this work, the probable coupling strengths depend on the lipid ratios on each layer. The coupling ranges estimated from our work differ from the ranges reported in previous works. We have predicted the domain coarsening dynamics for the symmetric and asymmetric cases. The scaling law is $R(t) \sim t^n$ where $n \approx 1/3$ for symmetric case and $n \approx 0.3$ for asymmetric case. The scaling law in the power-law of time agrees with previous computational works but it differs from the values of the growth exponent.

ACKNOWLEDGEMENTS

This work is partially supported by Faculty of Science, Mahidol University, the Center of Excellence for Innovation in Chemistry (PERCH-CIC), the Thailand Center of Excellence in Physics (ThEP), the Thailand Research Fund (TRF), the Commission on Higher Education (CHE), and the Development Promotion of Science and Technology (DPST), Thailand.

REFERENCES

Almeida PFF (2009). Thermodynamics of lipid interactions in complex bilayers. Biochim. et Biophys. Acta (BBA)-Biomembranes 1788:72-85.

Camley BA, Brown FLH (2011). Dynamic scaling in phase separation kinetics for quasi-two-dimensional membranes. J. Chem. Phys. 135:2251065.

Collins MD, Keller SL (2008). Tuning lipid mixtures to induce or suppress domain formation across leaflets of unsupported asymmetric bilayers. Proc. Nat. Acad. Sci. 105:124-128.

Collins MD (2008). Interleaflet coupling mechanisms in bilayers of lipids and cholesterol. Biophys. J. 94:32-34.

Ehrig J, Petrov EP, Schwille P (2011). Phase separation and near-critical fluctuations in two-component lipid membranes: Monte Carlo simulations on experimentally relevant scales. New J. Phys. 13:045019.

Gómez J, Sagués F, Reigada R (2008). Use of an enhanced bulk diffusion-based algorithm for phase separation of a ternary mixture. J. Chem. Phys. 129:184115.

Hohenberg PC, Halperin BI (1977). Theory of dynamic critical phenomena. Rev. Mod. Phys. 49:435-479.

Honerkamp-Smith AR, Cicuta P, Collins MD, Veatch SL, Den Nijs M, Schick M (2008). Line tensions, correlation lengths, and critical exponents in lipid membranes near critical points. Biophys. J. 95:236-246.

Honerkamp-Smith AR, Veatch SL, Keller SL (2009). An introduction to critical points for biophysicists; observations of compositional heterogeneity in lipid membranes. Biochim. et Biophys. Acta (BBA)-Biomembranes 1788:53-63.

Kiessling V, Wan C, Tamm LK (2009). Domain coupling in asymmetric lipid bilayers. Biochim. et Biophys. Acta (BBA)-Biomembranes 1788:64-71.

Laradji M, Kumar PBS (2004). Dynamics of domains growth in self-assembled fluid vesicles. Phys. Rev. Letts. 93:198105.

Laradji M, Kumar PBS (2006). Anomalously slow domain growth in fluid membranes with asymmetric transbilayer lipid distribution. Phys. Rev. E. 73:040901.

Liang X, Li L, Qiu F, Yang Y (2010). Domain growth dynamics in multicomponent vesicles composed of BSM/DOPC/cholesterol. Physica A: Stat. Mech. Appl. 389:3965-3971.

May S (2009). Trans-monolayer coupling of fluid domains in lipid bilayers. Soft Matter. 5:3148-3156.

Onsager L (1944). Crystal statistics. I. A two-dimensional model with an order-disorder transition. Phys. Rev. 65:117-149.

Putzel GG, Uline MJ, Szleifer L, Schick M (2011). Interleaflet Coupling and Domain Registry in Phase-Separated Lipid Bilayers. Biophys. J. 100:996-1004.

Risselada HJ, Marrink SJ (2008). The molecular face of lipid rafts in model membranes. Proc. Nat. Acad. Sci. 105:17367-17372.

Ramachandran S, Komura S, Gompper G (2010). Effects of an embedded bulk fluid on phase separation dynamics in a thin liquid film. Eur. Phys. Letts. 89:56001.

Saeki D, Hamada T, Yoshikawa K (2006). Domain Growth Kinetics in a Cell-sized Liposome. J. Phys. Soc. Jpn. 75:013602.

Veatch SL, Keller SL (2002). Organization in lipid membranes containing cholesterol. Phys. Rev. letts. 89:268101.

Veatch SL, Keller SL (2003). Separation of liquid phases in giant vesicles of ternary mixtures of phospholipids and cholesterol. Biophys. J. 85:3074-3083.

Veatch SL, Keller SL (2005). Seeing spots: complex phase behavior in simple membranes. Biochim. Biophys. Acta. (BBA)-Mol. Cell Res. 1746:172-185.

Wagner AJ, Loew S, May S (2007). Influence of monolayer-monolayer coupling on the phase behavior of a fluid lipid bilayer. Biophys. J. 93:4268-4277.

Wan C, Kiessling V, Tamm LK (2008). Coupling of cholesterol-rich lipid phases in asymmetric bilayers. Biochemistry 47:2190-2198.

Yanagisawa M, Imai M, Masui T, Komura S, Ohta T (2007). Growth dynamics of domains in ternary fluid vesicles. Biophys. J. 92:115-125.